Colloids and Surfaces A: Physicochemical and Engineering Aspects 697 (2024) 134466

Contents lists available at ScienceDirect

Colloids and Surfaces A: Physicochemical and Engineering Aspects

journal homepage: www.elsevier.com/locate/colsurfa

Types of phases obtained by molecular dynamics simulations upon freezing of hexadecane-containing systems

Sonya Tsibranska [a], Stoyan Iliev [b], Anela Ivanova [b,*], Nikola Aleksandrov [a], Slavka Tcholakova [a], Nikolai Denkov [a]

[a] Department of Chemical and Pharmaceutical Engineering, University of Sofia, 1 James Bourchier blvd, Sofia 1164, Bulgaria
[b] Department of Chemical and Pharmaceutical Engineering, Faculty of Chemistry and Pharmacy, University of Sofia, 1 James Bourchier blvd, Sofia 1164, Bulgaria

HIGHLIGHTS

- The cooling rate effect on rotator phases formation in hexadecane is traced by MD.
- Hexadecane exhibits multiple rotator phases upon freezing.
- Slower cooling yields larger main crystallites in bulk or at an interface.
- Thermodynamic and structural parameters quantify the degree of ordering.
- The phase state of the systems is identified with a set of structural descriptors.

GRAPHICAL ABSTRACT

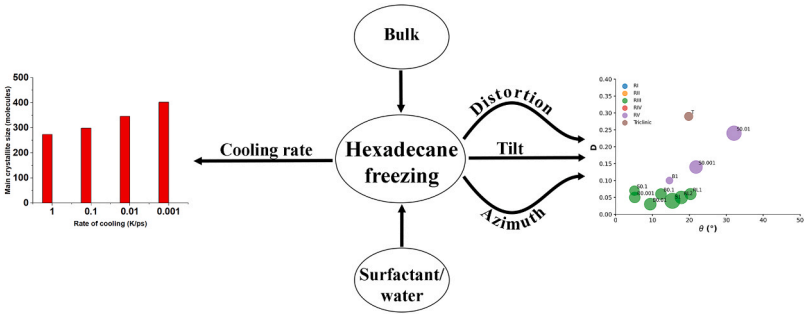

ARTICLE INFO

Keywords:
Hexadecane
Rotator phase identification
Molecular dynamics
Cooling rate
Structural analysis

ABSTRACT

Medium- to long-chain alkanes can form upon cooling intermediate phases between isotropic liquid and solid crystalline, called rotator phases, where relative freedom of the molecules to rotate about their long axis is combined with long range translational order. Rotator phases are well documented experimentally but the mechanism of their formation at the molecular level is still not fully explained. In a previous work, we have shown that molecular dynamics simulations can produce rotator phases upon cooling of hexadecane [S. Iliev et al., J. Col. Int. Sci., 2023, 638, 743]. The aim of the current work is to develop a procedure to identify the specific ordered phase obtained in the simulations. The influence of the cooling rate on the freezing process of hexadecane (bulk and surfactant-interfaced to water) is tested as well. Several parameters are combined to quantify the degree of ordering and the type of phase in the studied systems. These are the tilt angle of the molecules with respect to the crystallite plane, the radial distribution function of the centre of mass of the molecules in the crystallite, the percentage of the *gauche* torsion angles in the molecules, the angle of the second principal axis of each molecule with respect to the *x* axis of the coordinate system, and estimates from Voronoi analysis. The results show that the systems form a rotator phase, which transitions gradually towards the thermodynamically most stable triclinic crystal, and the transformation progresses to different extent depending on the system. The influence of the cooling rate is related only to the size of the largest crystallite formed, the other parameters of the freezing process remain unaffected. The work also presents a robust procedure for obtaining and identifying different types of ordered phases in alkane-containing systems with thoroughly tested

* Corresponding author.
E-mail address: aivanova@chem.uni-sofia.bg (A. Ivanova).

https://doi.org/10.1016/j.colsurfa.2024.134466
Received 7 February 2024; Received in revised form 31 May 2024; Accepted 3 June 2024
Available online 4 June 2024
0927-7757/© 2024 The Authors. Published by Elsevier B.V. This is an open access article under the CC BY-NC license (http://creativecommons.org/licenses/by-nc/4.0/).

computational protocol and a comprehensive set of structural analyses. Several key characteristics are advanced, compared to previous research [Ryckaert et al., Mol. Phys., 1989, 67, 957; Wentzel et al., J. Chem. Phys. 2011, 134, 224504], namely, a new methodology is proposed to compute the unit cell deformation parameter and azimuthal angle from MD simulation trajectories of the freezing process in alkane-containing systems. The suggested structural analysis, which is independent of the coordinate system, is applicable to any linear-chain system with polycrystalline structure.

1. Introduction

Alkanes in bulk and in mixtures with surfactants can form intermediate structural phases in a temperature range between an isotropic liquid and a regular solid crystalline phase [1,2]. These intermediate phases are commonly known in the literature as "rotator phases" or "plastic phases". They are characterised with the ability of the molecules therein to rotate about their long molecular axis, while retaining their long-range positional order in 3D space (similar to crystal arrangements) and they also exhibit complex visco-plastic rheological behaviour [3].

There are five rotator phases of alkanes (denoted R_I to R_V) described in the literature [4]. They are differentiated by the intermolecular arrangement, reflected in varying shape and/or distortion of the unit cell, and by the magnitude of the tilt of the molecules with respect to a crystal plane.

The properties of rotator phases have been extensively studied experimentally [4–14]. It has been shown that the formation of thermodynamically stable rotator phase is highly dependent on whether the alkane is odd- or even numbered. For alkanes with odd number of carbon atoms in the chain, 11 C atoms are enough to achieve thermodynamic stability of the intermediate phase, while for even numbered alkanes this is observed at 22 C atoms or more [14]. For bulk $C_{16}H_{32}$, a transient rotator phase is registered experimentally [13]. The type of crystal lattice formed after the rotator phase transforms into a crystal is also influenced by both the parity of the alkane and the chain length. For odd-numbered alkanes, triclinic and orthorhombic crystal lattices are observed, while for even-numbered alkanes, triclinic, monoclinic and orthorhombic lattices are formed [15]. Hexadecane freezes in a triclinic lattice [15].

Confining alkanes to micro- or nano structures can greatly affect the phase transition temperature and the stability of the rotator phases formed [13]. Furthermore, shorter alkanes exist in metastable or stable rotator phases at these conditions that are typical only for much longer alkanes. The extreme reduction in the volume available for the alkane and the presence of surface curvature also influence the type and rate of crystallisation with the latter being significantly increased when a rotator phase is formed [16,17].

The properties of rotator phases are also studied in a number of molecular simulation studies [18–48]. Most of the studies start from an idealised rotator phase of a single alkane or a mixture of alkanes. The studied property is either the melting point of the constructed phase or its stability at certain conditions. Hexadecane is rarely studied computationally [35,48]. In both works, hexadecane is determined to be the most stable in the triclinic phase, which is in agreement with the experimental data [14]. The effect of the cooling rate on the freezing process has not been monitored yet.

Some of the studies investigate the solid-solid transitions between the various rotator phases or to the crystal phase. Cao et.al. [34] study the miscibility of binary mixtures of n-alkanes (from hexane to octane) with hard sphere Monte Carlo simulations. The same authors also investigate the phase behaviour of n-alkanes with varying chain lengths (between 9 and 21 carbon atoms) [35]. For the modelled systems with even parity with chain length of 18 carbon atoms or shorter, it is found that the triclinic phase is the most stable. However, for the system with $C_{20}H_{42}$ both monoclinic crystal structure and a rotator phase are detected and the transition between them is monitored.

Marbeuf et al. [36] simulate with molecular dynamics systems containing $C_{18}H_{38}$ – $C_{20}H_{42}$ in NσT ensemble at various pressure. Spontaneous formation of R_I phase is observed in the $C_{19}H_{40}$ system at 300 K which aligns with the experimental data. The authors observe that the molecular rotation is achieved by a "jump" of the molecule followed by 90° rotation about the long axis. This phenomenon was also observed in previous studies of Ryckaert et al. [23–2425].

Wentzel et al. [37,38] perform MD simulations of $C_{23}H_{48}$ and a mixture of $C_{21}H_{44}/C_{23}H_{48}$ with length of 1 ns. Several all-atom force fields are tested with Flexible Williams [49] best replicating the experimental data. In their work, they achieve a sequence of phases: orthorhombic crystalline, R_I, R_{II}, and melt. The solid transitions are monitored by newly defined Potts- and Ising-like order parameters.

Milner et al. [39] carry out all-atom MD simulations of $C_{23}H_{48}$ and polyethylene. The molecular conformation, mobility, formation energy, and fluctuation free energy of twist solitons are studied. To calculate the orientation of the twists, an order parameter indicating the orientation of the atoms in the molecule is proposed. The energy of formation for each ordered phase is calculated, with that of R_{II} being the lowest.

The results of the simulation studies described thus far are based on relatively short simulations (up to 2 ns). Furthermore, the starting structure for the simulations is either idealised crystalline structure or idealised rotator phase that is heated until melting or monitored at given conditions. These imposed conditions do not allow evaluation of the mechanism of formation of rotator phases. Also, in these studies the type of ordered phase is determined by just one or two order parameters, while by definition the rotator phases are characterised by up to four different order parameters [2]. It is also noteworthy that none of the previous computational works addresses alkanes at surfactant-stabilised interface with water.

In our previous works, we have established a robust computational protocol for simulation of alkane-containing systems in bulk and at a surfactant-stabilised water interface [50]. We have also carried out some preliminary analysis on the phase state of the studied systems. It was concluded that in bulk the mechanism of the freezing process is stochastic, and at the interface freezing is induced by templating of the surfactant molecules. A computational procedure to determine the phase state of crystallites consisting of quasilinear molecules has been proposed [51].

In the current study, we investigate the freezing process in two types of alkane-containing systems: bulk hexadecane and hexadecane at a flat surfactant-stabilised interface with water. The effect of the rate of cooling is monitored. Thermodynamic characteristics are analysed to determine the type of phase transition taking place in the systems. The degree of ordering of the frozen systems is quantified with radial distribution functions (RDF), percentage of *gauche* conformations in the crystallites and rotational freedom about the long axis of the molecules. The phase state of the formed crystallites is classified by a combination of three structural parameters, namely: tilt angle (θ) of the molecules with respect to the crystallite plane, degree of distortion of the hexagonal lattice (D) and azimuthal angle (Φ_d).

The combination of the proposed computational protocol and the developed methodology for structural analysis builds upon the existing research in several key characteristics [18–48]. The utilised force field has a relatively modest computational cost, hence, allowing more extensive simulation times which are essential for the observation of longer phase transitions. Additionally, there is no bias introduced in the simulations, which enables the systems to undergo a natural transition

from liquid to solid state. The methodology used in the study can determine rigorously the phase state of crystallites in a polycrystalline system without the need for the crystallites to be oriented in a specific way. Finally, the structural parameters for determining the phase state are identical with the ones used in the experiment [18,23,24,48]. This enables straightforward comparison between solid state phases in alkane-containing systems obtained from experiments and from simulations.

2. Material and methods

The results obtained in this paper are based on two types of model systems. The first one consists of 440 molecules (22,000 atoms) of bulk hexadecane (denoted further on as bulk HEX) (Fig. 1, A), and the second one contains 494 molecules hexadecane and 108 surfactant $C_{16}(EO)_2$ molecules arranged at a flat water interface (2778 water molecules) (Fig. 1, B). The latter system has ≈43,000 atoms and it will be denoted further on as HEX/Surf/water.

The starting structures of both systems are ordered. The molecules are placed on the nodes of a regular hexagonal lattice and each of them is rotated randomly about the long molecular axis to accelerate melting. Exact details about the construction of the models are given in our previous work [50].

The energy of the two model systems is minimised first. Then, they are heated to 350 K with a rate of 1 K/ps in NVT ensemble and equilibrated at this temperature for 200 ns in NPT ensemble (P = 1 bar). After this stage, a fully isotropic liquid is achieved, which is used as initial configuration for all subsequent MD simulations. Starting from the final snapshot at 350 K, the systems are cooled down to 300 K and again equilibrated for 200 ns at the respective lower temperature with the same computational parameters. After the systems are equilibrated at 300 K, they are cooled down to 278 K at four different cooling rates (1 K/ps, 0.1 K/ps, 0.01 K/ps or 0.001 K/ps) to establish if there is an effect of the cooling rate on the formation and the type of the ordered phase obtained in the systems after freezing. For achieving statistical significance of the sampling, each system is simulated in three independent configurations, differing in the initial velocities for the cooling stage, thus totalling 24 independent trajectories. The final target temperature of 278 K is chosen as a result of benchmarking done in a previous study [50].

Each of the cooled down systems is simulated for 1000 ns in NPT ensemble with isotropic (bulk hexadecane) or semi-isotropic (HEX/Surf/water) pressure scaling with P = 1 bar in all directions. The thermostat and barostat are v-rescale [52] and Berendsen [53], respectively. The potential for the van der Waals interactions is Lennard-Jones and is truncated at a distance of 1.2 nm with a switching function activated at 1 nm. The electrostatic interactions are calculated with PME [54–57], where the direct summation is truncated at 1.2 nm with a switching function turned on at 1.0 nm. The time step is 2 fs, and the equations of motion are integrated with leap-frog. The lengths of all hydrogen-containing bonds are fixed with LINCS [58] and those in water – with SETTLE [59]. Coordinates are written every 10 ps to the trajectory file. A hexagonal periodic box is used for all simulations with initial dimensions 5.2 ×4.5 ×9 nm for bulk hexadecane and 5.2 ×4.5 ×17.2 nm for the hexadecane/surfactant/water system. The force field used is CHARMM36 [60] in combination with TIP4P [61,62] water model. The chosen force field was verified to produce results consistent with the experiments in a previous work [51].

Two reference systems of bulk HEX in triclinic and rotator (R_I) phase were also built and simulated for 1000 ns with the same parameters as the model systems. The reference crystals were constructed from experimental data [13] and were simulated directly at 278 K to avoid melting.

The MD simulations are carried out with the programme package Gromacs 2020 [63]. VMD 1.9.4 [64] is used for visualisation of the trajectories. Built-in Gromacs tools and self-written tailored scripts [51] are employed to perform the data analyses.

3. Results and discussion

3.1. Global structuring and representative crystallites

After 1 ns MD simulation at 278 K all investigated trajectories exhibited a polycrystalline structure, independent of the cooling rate. The composition of each model system at the end of the production simulation is presented in the Supplementary Material (SM, Table S1). To structurally analyse the ordered phases in our systems, the individual crystallites are first isolated. The methodology for isolation and the procedure for the analyses done on the isolated crystallites are described in detail in our previous publication [51].

For each cooling rate, a large representative crystallite is fully analysed for bulk HEX and HEX/Surf/water, totalling 8 separate crystallites. All of the structural analyses described below are done for the last 100 ns of the production simulation. Two of the crystallites (one for each model

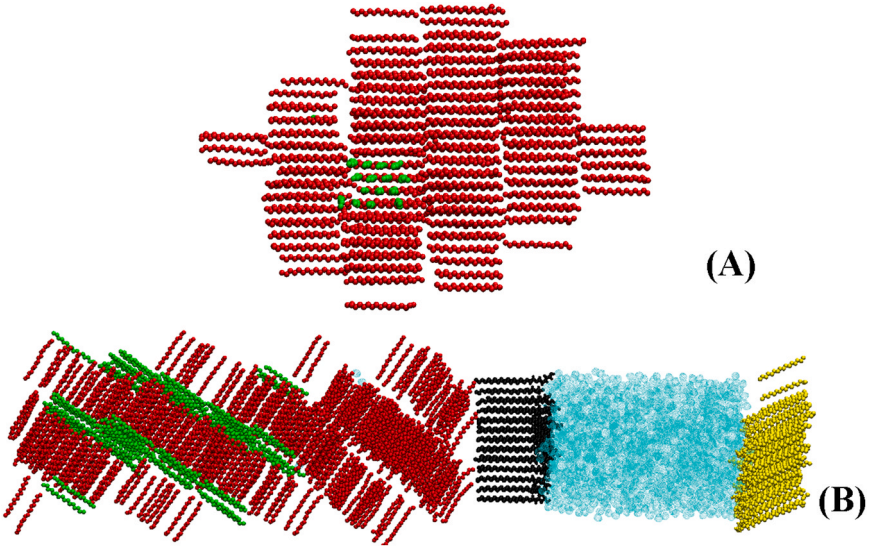

Fig. 1. The two types of model systems used in the study: (A) Bulk HEX and (B) HEX/Surf/water, illustrated with the snapshots after 1 μs molecular dynamics at 278 K reached with cooling rate of 1 K/ps. Each of the formed crystallites is coloured differently; water is cyan.

system) are presented in Fig. 2 and the rest are summarised in the SM, Figure S1.

Before analysis of the obtained structures, the type of phase transition occurring in the systems upon cooling should be determined. This can be done by interpreting the evolution of the enthalpy profiles of the systems during the simulations. Furthermore, transitions from liquid to solid are characterised by change in the density of the respective system.

3.2. Analysis of the enthalpy and density profiles of the systems

First order transitions are characterised by a sharp drop (in the case of freezing) in the enthalpy of the system. This phenomenon is observed in all of the model systems indicating that the transition from liquid to solid is of first order. The time at which it takes place can vary between the systems and does not depend systematically on the cooling rate.

The quantitative enthalpy change can be a good initial indicator of the phase state of the systems. Cholakova et al. [13] show that 65–80 % of the total phase transition enthalpy can be attributed to the formation of a rotator phase. This range is determined from significant amount of experimental data available for alkanes with chain length between 10 and 29 carbon atoms. The transition enthalpy is obtained from differential scanning calorimetry experiments. The studies show that on average the first-order transition from liquid to the initially formed rotator phase accounts for 2/3–4/5 of the transition enthalpy to a triclinic crystal. The enthalpy differences between the liquid and the solid phase in the studied systems and their ratios with the experimental data for a transition from liquid to triclinic phase in bulk HEX are given in Fig. 3. The numerical data are summarised in Table S2.

Most of the systems feature decrease in their enthalpies in the expected range for a transition to a triclinic phase going through a rotator phase, with three main exceptions, namely bulk HEX at 0.001 K/ps, HEX/Surf/water at 0.01 K/ps and HEX/Surf/water at 0.001 K/ps. These three systems have enthalpies decreased by more than 80 % of the experimental enthalpy for a transition from liquid to triclinic phase of bulk HEX. This indicates that these three models have advanced towards a triclinic phase more than the others where the share of rotator phase seems to be significant. This assumption may be verified further by structural analysis.

As the systems transition from liquid to solid state, while their enthalpies decrease, the densities are expected to increase. Thus, an inverse correlation between these two properties is expected. Plotting the transition enthalpies as function of the densities measured at the end of the simulations does indeed reveal such linear correlation with R^2 of 0.93 (Figure S2, A). Furthermore, we investigated whether the number of frozen molecules in a given model contributes to an increased density. Indeed, a significant linear correlation is found with R^2 of 0.96 (Figure S2, B). A molecule is considered frozen if the distance between the C3 and C14 atoms along the alkyl chain (Fig. 4) is persistently $\geq$1.4 nm [51] during the last 100 ns of the simulation.

To evaluate the effect of the cooling rate on the freezing of the systems, we calculated the percentage of the number of molecules in the largest crystallite at every cooling rate. The data are presented in Fig. 4 and outline a clear trend – a slower cooling rate induces the formation of larger crystallites even though from an experimental point of view all cooling rates are extremely fast. This coincides with the first-principles expectations of crystallisation theory.

As pointed out at the beginning, to establish the type of ordered phase of the studied crystallites, multiple parameters are required. As a

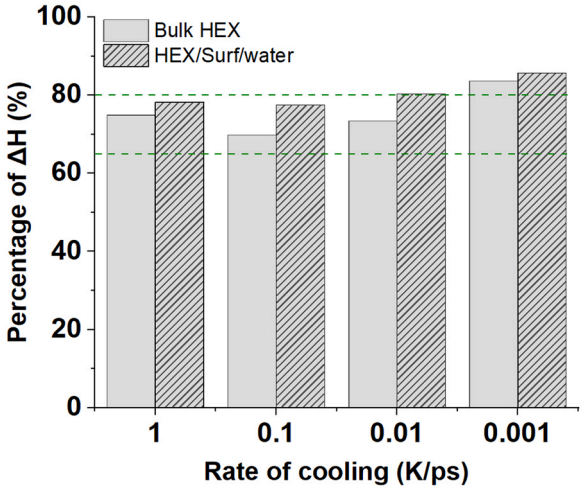

Fig. 3. Relative enthalpy decrease in the model systems after transition from liquid to solid state given as percentage of the total enthalpy (ΔH) for transition of bulk HEX to a triclinic crystal [13].

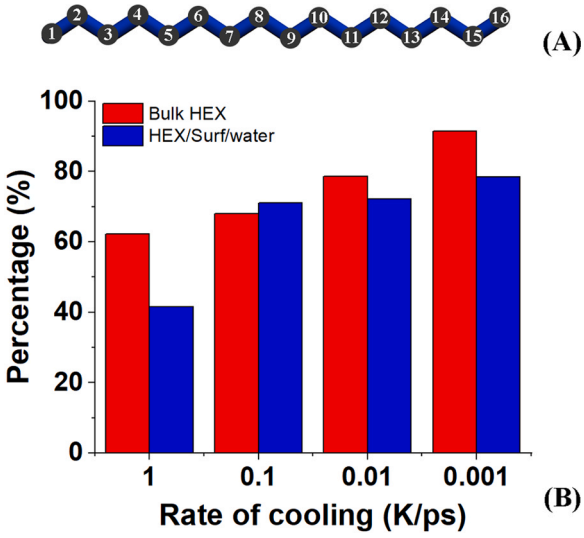

Fig. 4. (A) Numbering of the carbon atoms in the hexadecane molecule and (B) percentage of molecules in the largest crystallite at each cooling rate. The percentages for the HEX/Surf/water systems are calculated only from the number of hexadecane molecules to allow direct comparison with the bulk HEX systems.

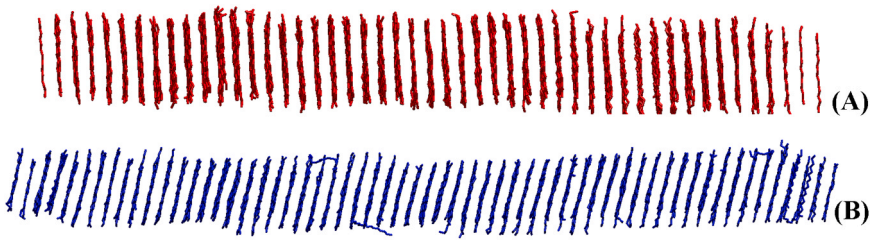

Fig. 2. Illustration of two of the studied crystallites after processing to reconstruct the real-space coordinates of the molecules with the procedure proposed in our previous work [51]; (A) Bulk HEX at 0.001 K/ps and (B) HEX/Surf/water at 0.001 K/ps.

first step, the ratio of the *gauche* torsion angles C-C-C-C in the alkyl chains of all molecules in each representative crystallite is calculated.

3.3. Gauche/trans ratio in the crystallites

As the molecules transition from a liquid to a crystalline structure, their freedom of movement is limited and the energy cost for a conformational change increases. Thus, a decrease in the *gauche* conformations indicates higher ordering [36]. To differentiate more precisely the degree of ordering of the molecules in the representative crystallites, three types of torsion angles were examined: containing a terminal methyl group (these groups have the highest freedom of mobility), containing a terminal methylene group (the second (C2) and fifteenth (C15) carbon atoms for hexadecane) and containing internal methylene groups. The percentages of *gauche* conformations in each crystallite and in the two reference systems for the three categories of torsion angles, averaged over the last 100 ns of the simulation, are presented in Fig. 5.

The values are calculated by means of a histogram constructed by counting the torsion angles in the three parts of each molecule separately (Fig. 5). The total area of each histogram is normalised to 1. Thus, measuring the area of the histograms in the range from −135° to 135° yields the fraction of *gauche* conformations for the respective fragment of the molecule.

It is evident that the internal parts of the molecules in all crystallites and the reference systems are all in *trans* conformation for the analysed time period. Some variance is observed in the ratio for the terminal methylene groups but the differences are small. However, the strongest indicator of the degree of ordering is the percentage of *gauche* conformations in the methyl groups. Most of the systems exhibit a significantly higher degree of mobility in the methyl groups compared to the reference triclinic phase and have relatively close values to the rotator phase. It is noteworthy that in a previous study [50] the reference rotator phase system was determined to be in a state of transition to a triclinic phase towards the end of the simulation. Bulk HEX at 0.1 K/ps presents the highest degree of disorder (Table S3) among the systems in this analysis. However, this can be attributed to a period of active transition to crystalline phase which is supported by the rest of the analyses *(vide infra)*. HEX/Surf/water at 0.01 K/ps, on the other hand, has the lowest percentage of *gauche* conformations across the sets (Table S3). This indicates that the system is in an advanced stage of transitioning towards a triclinic crystalline phase, although it is not yet fully ordered.

In earlier publications, the change in *gauche* conformation has been used as an indicator of the phase transition from crystal to rotator phase

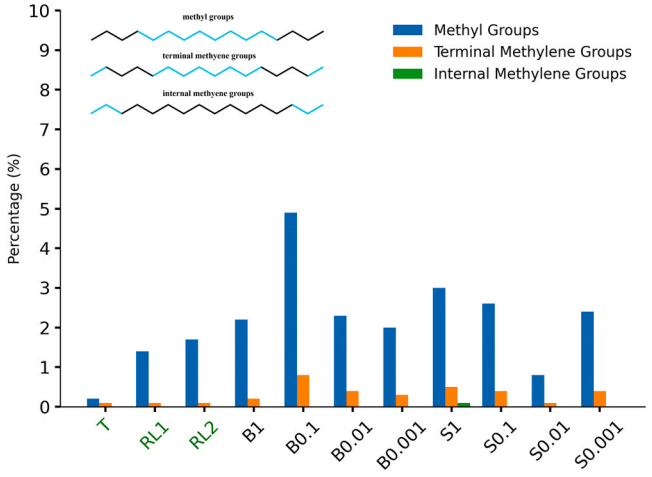

Fig. 5. Percentage of *gauche* conformations in the studied crystallites and the two reference systems. The three types of torsion angles (in black) calculated for each molecule in the crystallites are denoted in the upper left corner. RL1 and RL2 stand for each of the two layers of the reference rotator crystal.

[36], and between crystal and liquid phases [48]. Marbeuf & Brown detected the transition from orthorhombic crystalline phase to R_I in $C_{19}H_{40}$ by a sudden increase in the *gauche* conformations causing a decrease in the *c* parameter in the unit cell. Burrows et al. detected the melting and freezing temperatures in systems of $C_{16}H_{34}$ and $C_{15}H_{32}$ by continuously heating or cooling their systems until a sudden change in the number of *gauche* conformations was present, which indicated the transition. In this report, however, only gross division of the *trans* and the *gauche* conformations between liquid and solid state was done.

It may be concluded that the percentage of *gauche* conformations in the crystallites is a sensitive indicator of their degree of ordering. However, the analysis does not provide any information about the local packing of the molecules and also about the type of rotator phase. A popular method to quantify the local intermolecular arrangement is to calculate the radial distribution functions (RDF).

3.4. Analysis of the radial distribution functions of the crystallites

The RDFs between the centres of mass of the molecules in the crystallites and the two reference systems are calculated and scaled by the volume of the respective system and the number of molecules in the crystallite to allow comparison. Since each crystallite consists of a different number of molecules and the systems vary in volume, the intensities of the RDF peaks are not directly comparable unless properly scaled. Thus, an additional scaling factor is applied to the intensities of all RDFs. This factor scales the volume of each system by a reference volume (in our case the volume of the system of bulk HEX at 1 K/ps) and the number of molecules in each crystallite are divided by the total number of hexadecane and surfactant molecules in the respective system. After the additional scaling is applied, the RDF profiles are directly comparable.

To quantitatively establish how similar each crystallite is to either of our reference systems, the Jaccard index is calculated [65]. The index can vary in the range from 0 to 1, where 0 means the two profiles have no overlap and 1 – that they are identical. Before calculating the index, the RDFs are truncated at 1.5 nm since the tails of the function can become noisy and cannot be interpreted reliably. The calculated Jaccard indices are presented in Table 1.

Similar to the previous analysis, most of the crystallites show strong resemblance to the reference rotator phase system. The systems that are in an active transition to triclinic phase (bulk HEX at 0.1 K/ps; HEX/Surf/water at 0.01 K/ps and 0.001 K/ps) have a drastically lower Jaccard index with the rotator phase relative to the rest of the crystallites. Comparing the transitioning structures with the reference triclinic phase reveals a slight but significant increase in similarity. A visual inspection of the RDF profiles (Figures S3, S4) can explain this behaviour.

The two reference systems differ mainly in their first peak. The rotator phase is characterised by a single intensive peak, while the triclinic phase has three closely spaced narrow peaks, each less intensive than the previous.

Table 1
Jaccard indices calculated from comparison of the RDF profiles of each crystallite with those of the two reference systems.

System	Triclinic	R_I→T
R_I→T	0.34	1.00
Bulk HEX		
1 K/ps	0.35	0.82
0.1 K/ps	0.39	0.45
0.01 K/ps	0.30	0.72
0.001 K/ps	0.33	0.80
HEX/Surf/water		
1 K/ps	0.34	0.82
0.1 K/ps	0.34	0.76
0.01 K/ps	0.39	0.30
0.001 K/ps	0.39	0.51

The three crystallites (bulk HEX at 0.1 K/ps (Figure S3, C, D) and HEX/Surf/water at 0.01 K/ps (Figure S4 E, F), and 0.001 K/ps (Figure S4, G, H)) have two separate first-neighbour peaks. These are very well defined in the two HEX/Surf/water crystallites while the peak separation in the bulk HEX crystallite is still small. The formation of these peaks contributes to the increased similarity of the three crystallites with the triclinic phase. However, the positions of the peaks are still shifted to higher distances, their intensities are lower, and the width of the peaks is larger than that in the triclinic phase, which accounts for the relatively low degree of overlap between the RDF profiles of the three crystallites and the triclinic phase.

The rest of the crystallites all show initial stages of separation of the first peak into multiple ones. However, they all still follow very well the profile of the reference rotator phase.

Hence, the RDF profiles are vital for determining the phase state of the crystallite and the extent of transition to the final crystal. Quantifying how similar each crystallite is to the two reference systems separates them in two groups. Bulk HEX at 0.1 K/ps and HEX/Surf/water at 0.01 K/ps and 0.001 K/ps are in an active transition towards a triclinic phase. Bulk HEX at 0.1 K/ps is still in the early stages of the transition, while HEX/Surf/water at 0.01 K/ps is the closest to a triclinic phase. The rest of the crystallites remain very similar to the reference rotator phase.

As mentioned at the beginning of the paper, the main difference between a rotator phase and a crystalline phase is the ability of the molecules to pivot about their long axis. To quantify this degree of freedom, we calculate the angle of the second principal axis (P_2) of each molecule in the respective crystallite with the *x* axis of the coordinate system during the last 100 ns of the simulations.

3.5. Analysis of the angle of P_2 with the *x* axis of the coordinate system

In order to measure the desired angle, each crystallite is rotated so that the long axis of its molecules becomes parallel to the *z*-axis of the coordinate system. Thus, P_2 describes the bond orientations of the molecules in the *xy* plane. We first calculate the evolution of the angle between P_2 and the *x* axis for all molecules in each crystallite. The angle magnitudes are then counted in a histogram with bin width of 1° and normalised by the number of values. Thus, the histogram has a meaning of a probability distribution. In a structure where all molecules are completely immobile, the outcome of the analysis will be a delta function centred at 0°. In a simulated crystalline structure, the molecules are expected to oscillate slightly due to the thermal motion, so there would be a small spread around 0°. In contrast, crystallites in a rotator phase should have a measurably larger dispersion of the values.

To quantify the dispersion of the angles, the central peaks of the histograms are fitted to a Gaussian function. The standard deviation of each fit is used as an indicator of the freedom of rotation. The values for all systems are presented in Table 2.

Table 2
Standard deviations of the Gaussian fits to the calculated histograms of the evolution of the angle between P_2 and the *x* axis of the coordinate system in the representative crystallites.

System	Standard deviation (°)
Triclinic crystal	8
$R_I \rightarrow T$ layer 1	10.5
$R_I \rightarrow T$ layer 2	11
Bulk HEX	
1 K/ps	11
0.1 K/ps	13.5
0.01 K/ps	11.5
0.001 K/ps	11.5
HEX/Surf/water	
1 K/ps	11
0.1 K/ps	11
0.01 K/ps	7.5
0.001 K/ps	11

All of the systems except HEX/Surf/water at 0.01 K/ps have standard deviations close to the ones of the model rotator phase. The former appears to be very close to a triclinic phase. However, inspection of the profile of the histogram (Figure S6, F) reveals two intensive peaks at ±180°, indicating that a large number of molecules have completed a full revolution during the 100 ns period. Thus, an active transition is still taking place during the analysed period. In contrast, the profile of the reference triclinic phase (Figure S5, A) has a single intensive peak centred at 0° and no satellite peaks.

Bulk HEX at 0.1 K/ps also exhibits a non-trivial number of molecules rotating during the studied period (Figure S6, C). The rotation is by ±80° and the main peak is characterised with the largest spread of values, hence, its relatively wide standard deviation. These results along with the rest of the analyses until now suggest that this system has a high degree of order. However, it is in a state of an active transition towards another solid phase, best illustrated by the increased similarity of its RDF profile with the RDF profile of the triclinic reference system (Table 1).

The rest of the systems are very well described by their peak centred at 0° degrees and a satellite peak with low intensity, similar to the profiles in the reference rotator phase (Figure S5, B, C).

The analyses shown thus far have elucidated very well the degree of ordering in the model systems compared to the reference ones. Some of the systems are still in the initial stages of their transition to a solid crystalline structure, while others have advanced much farther. However, these data are not sufficient to determine the precise phase of the studied crystallites. As mentioned at the beginning of the paper, the phase state of an alkane-containing crystal can be determined by a combination of structural parameters that will be detailed in the next section.

3.6. Phase state of the systems

There are three structural parameters (Fig. 6) that can unequivocally determine the phase state of each of our systems: distortion (D) of the hexagonal packing, which is calculated as 1 – A/B, where A and B are the short and long axes of an ellipse; azimuthal angle (Φ_d) describing the displacement of the first neighbours from the long ellipse axis; tilt angle (θ) of the molecules with respect to the crystallite plane [13].

The combination of these parameters, defining each phase, is presented in Table 3.

It is evident (Table 3) that each phase has a unique combination of the three parameters. To determine the phase state of our systems, we ordered the importance of these parameters hierarchically. First, we determine the value of θ since this parameter can only be in two states: $\theta = 0$ and $\theta > 0$. After that, the values of D are discriminated between 0, small or large. The limiting magnitudes of the three categories are based on those calculated for the initial experimental structures of hexadecane in the triclinic crystal [66] and the orthorhombic R_I phase [13] and their values are given in Table S4. If $\theta > 0$ and $D \neq 0$, then Φ_d is differentiated between 0 or >0. If $D = 0$, then Φ_d is not applicable because the elementary unit is a regular hexagon. Finally, if D is large, then it is compared to D of the triclinic phase, which was calculated to be 0.24 in the initial triclinic crystal and ~0.29 in this reference system after 1 μs of MD simulation. The conditions stated here are organised in a decision tree shown in Fig. 7.

The phase states of both the reference systems and the studied crystallites are presented graphically in Fig. 8. The numerical values are given in Table S4.

The triclinic phase remains almost unchanged during the whole simulation. The reference rotator phase is determined to be R_{III} even though it was constructed as R_I initially. The transition from R_I to R_{III} begins almost instantly in the simulation with molecules tilting to ~19° which is comparable with the triclinic phase and D being relatively small. It is important to point out that experimentally the R_I phase transitions directly to R_V [13], albeit for longer-chain hydrocarbons. The

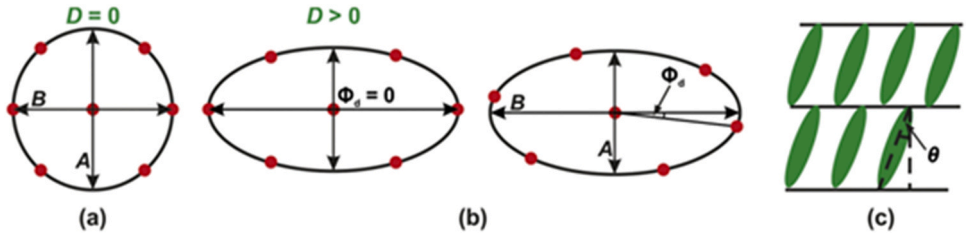

Fig. 6. Schematic representation of the structural parameters determining the phase state in alkane-containing systems: (a) distortion (D); (b) azimuthal angle (Φ_d); (c) tilt angle (θ).
Adapted from [13].

Table 3
Structural characteristics and type of crystal lattice of the rotator phases [2].

Phase	θ	D	Φ_d	Layer structure	Lattice
R_I	0	Large	0	ABABAB…	Face centred orthorhombic
R_{II}	0	0	-	ABCABC…	Rhombohedral
R_{III}	> 0	Small	> 0	AAA…	Triclinic
R_{IV}	> 0	Small	0	AAA…	Monoclinic
R_V	> 0	Large	0	ABABAB…	Face centred orthorhombic

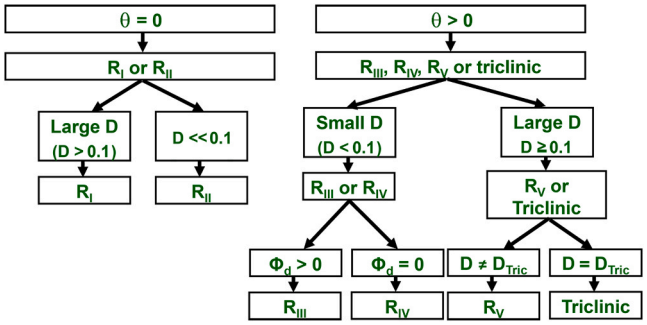

Fig. 7. Decision tree for determining the phase state of the studied crystallites, based on θ, D and Φ_d. R_x denote the various rotator phases.

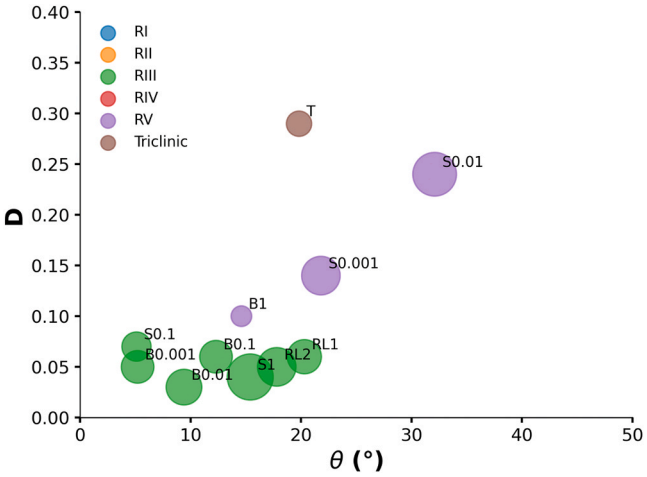

Fig. 8. Graphical representation of the phase states of the reference systems and the studied crystallites. B stands for bulk HEX, S – for HEX/Surf/water, RL1 and RL2 for rotator phase, layer 1 and layer 2, respectively, and T denotes the triclinic phase. Each colour represents a different phase, and the size of the circle reflects the magnitude of Φ_d. The cooling rates are given as numerical indices.

question arises then why the simulations predict the initial transition of HEX to be through R_{III}. There could be two reasons for that. It is possible that the transition to R_{III} takes place in a very short time interval, inaccessible to an experimental approach. The second reason might be the constrained size of the model systems which may favour the formation of a single layer structure (AAAA) in the crystallites and, hence, the respective phase (Table 3). All spontaneously frozen model systems indeed feature single-layer largest crystallites, which were analysed. However, the reference rotator phase is initially built as a R_I phase which has a double layer structure (ABAB, Figure S7, left). Thus, we can track the evolution of this structure through the 1 μs simulation time along direction *c* of the lattice (Figure S7). It is evident that even at 500 ns the structure already approaches an AAAA structure like in the R_{III} phase. This is maintained even further up to the end of the simulation of the reference system. This indicates that the appearance of the R_{III} phase is most likely a short-time event.

Most of the parameters of frozen model systems are comparable to those of the R_{III} rotator phase. However, they can vary substantially, which is explained by the different stage of the transition to the crystal, evidenced by the rest of the analyses discussed above. The crystallite from the HEX/Surf/water system at 0.01 K/ps is the one that was determined to be in most advanced transition from R_V to triclinic state. The molecules in this crystallite have very large θ and value for D that is close to the one in the triclinic phase. $\Phi_d > 0$, which is not typical for R_V. However, as stated above, the crystallite undergoes an active solid-solid transition towards the triclinic phase. There is one more system featuring $R_V \rightarrow T$ transition (Fig. 8, S0.001) but it is still at an earlier stage with respect to the deformation parameter D. Bulk HEX at 1 K/ps is the only crystallite in R_V phase.

The near-instant transition of the reference rotator phase system from R_I to R_{III} and the majority of the model systems being in R_{III} suggests that this is a possible phase for the hexadecane-containing systems. The overall classification indicates that there might be several paths for hexadecane, such as: liquid → R_{III} → R_V → triclinic or liquid → R_V → triclinic, or liquid → R_{III} → triclinic.

Even though R_{III} has not been detected experimentally in hexadecane, it is important to note that the processes studied here are at the microsecond scale with no bias in the simulations. It is evident that all of the studied systems, including the reference rotator phase, are in a state of transition and the observed phenomena are the initial packing events, leading ultimately to a triclinic crystalline phase. The obtained results indicate that there is also a possibility of other transition paths to take place in the initial very short time frame, which are too short-lived to be detected experimentally. None of the systems modelled in the current study are in a triclinic crystal by the end of the 1 μs simulations and at the same time significant enthalpy decrease takes place during the liquid to R_{III}/R_V first order transition. This still leaves room for possible additional transitions but most likely they would be of second order. Indeed, most of the rotator-rotator transitions are determined experimentally to be of second order [13].

4. Conclusions

In the current work, we study the liquid-solid phase transitions in hexadecane-containing systems. Two types of models are constructed – bulk hexadecane and hexadecane at a flat surfactant-stabilised interface with water. The systems are cooled down to 278 K, where they freeze, at four different cooling rates and then simulated by all-atom molecular dynamics for 1000 ns. The relatively long simulation time is necessary because there is no bias in the freezing process, which is a stochastic phenomenon, and it ensures enough time to observe and characterise the target transitions. The effect of the cooling rate is monitored. The degree of ordering is quantified by the percentage of *gauche* conformations in the crystallites and by radial distribution functions. The type of phase state is identified on the basis of three structural parameters.

Analysis of the thermodynamic characteristics of the systems confirms a first order transition from liquid to ordered state, which yields stochastically oriented polycrystalline samples. It turns out that the size of the largest crystallites in both types of model systems depends on the cooling rate. The models can be generally categorised in a state of transition from rotator to triclinic phase but progressing to different degree. Most of the systems (6 models) with significant overlap of the RDF to that of a reference rotator phase and relatively high percentage of *gauche* conformations in the terminal methyl groups are in an early transition stage. A noticeable split of the first RDF peak, albeit with large share of *gauche* conformations, is indicative of a stage of active transition (1 model). Completely split first peak in the RDF, aligning with those of the triclinic phase, and very low population of *gauche* conformations signifies more advanced progress toward the triclinic phase (1 model).

The rotational freedom of the molecules is evaluated through the angle between the second principal axis of the molecules and one of the coordinate axes. Two of the model systems feature a primary peak accompanied by two satellite maxima, revealing that the systems are in a state of transition toward the triclinic phase. The rest of the systems have one large peak and a small satellite, similar to the profile in the reference rotator phase.

The phase state of the studied crystallites and the reference systems is classified by the combination of three structural parameters, namely tilt angle relative to the crystallite plane, hexagonal unit cell distortion and azimuthal angle. These parameters are sorted hierarchically in a decision tree. The reference rotator phase is shown to have transitioned from R_I to R_{III} while the triclinic phase remains stable throughout the simulation. Most of the studied crystallites are in R_{III} phase with one being in R_V and two transitioning from R_V to the triclinic crystal. The near-instantaneous transition of the reference rotator phase confirms that hexadecane is stable in the triclinic state. The dynamics reveals that the transition to the latter phase is not direct, but there are a few fast transitions through rotator phases. The data suggest that there might be several transition paths for the hexadecane-containing systems: liquid → R_{III} → R_V → triclinic, liquid → R_V → triclinic, or liquid → R_{III} → triclinic.

Previously, the study of ordered phases in alkane-containing systems is generally done by constructing a model system in a predefined phase state [25,38,48]. This approach allows for shorter simulations to yield meaningful results, thus reducing computational time. However, this may also introduce bias. Traditionally, the phase state in the systems is monitored by one or two parameters. For example, Wentzel et al. define Ising and Potts-like parameters which are employed to differentiate between the R_I and R_{II} phases [38]. Ryckaert et al. monitor the tilt of the molecules with respect to the layer plane and the rotational disorder in the crystal [25]. There are two main limitations of this approach. First, the information from these analyses is not sufficient to differentiate between all possible rotator phases and, second, the analyses would depend on the orientation of the crystal. Our approach solves these problems by utilising a computational protocol that allows the systems to spontaneously form the ordered phase from a liquid state. Moreover, the subsequent analyses are orientation-independent. Finally, the combination of the three structural parameters discriminates between all five possible rotator phases and the triclinic crystal.

CRediT authorship contribution statement

Nikolai Denkov: Writing – review & editing, Validation, Funding acquisition, Conceptualization. **Sonya Tsibranska:** Writing – review & editing, Resources, Investigation, Formal analysis, Data curation. **Anela Ivanova:** Writing – review & editing, Supervision, Resources, Project administration, Methodology, Data curation, Conceptualization. **Stoyan Iliev:** Writing – review & editing, Writing – original draft, Software, Investigation, Formal analysis, Data curation. **Slavka Tcholakova:** Writing – review & editing, Validation, Project administration, Conceptualization. **Nikola Aleksandrov:** Software, Formal analysis.

Declaration of Competing Interest

The authors declare that they have no known competing financial interests or personal relationships that could have appeared to influence the work reported in this paper.

Data availability

Data will be made available on request.

Acknowledgements

This study was funded by the Bulgarian Ministry of Education and Science, under the National Research Program "VIHREN", project ROTA-Active (No. KP-06-DV-4/16.12.2019). This work was supported by a grant from the Swiss National Supercomputing Centre (CSCS) under project ID ch13 for the computational time. Dr. Diana Cholakova is acknowledged for providing data from experimental measurements and for assisting with their interpretation.

Appendix A. Supporting information

Supplementary data associated with this article can be found in the online version at doi:10.1016/j.colsurfa.2024.134466.

References

[1] D. Small, The Physical Chemistry of Lipids. From Alkanes to Phospholipids, Springer, New York, 1986. ISBN-13:؟ 978-0306417634.
[2] E. Sirota, H. King, D. Singer, H. Shao, Rotator phases of the normal alkanes: an x-ray scattering study, J. Chem. Phys. *98* (1993) 5809–5824, https://doi.org/10.1063/1.464874.
[3] D. Cholakova, K. Tsvetkova, S. Tcholakova, N. Denkov, Rheological properties of rotator and crystalline phases of alkanes, Colloids Surf. A Physicochem. Eng. Asp. *634* (2022) 127926, https://doi.org/10.1016/j.colsurfa.2021.127926.
[4] D. Cholakova, N. Denkov, S. Tcholakova, I. Lesov, S. Smoukov, Control of drop shape transformations in cooled emulsions, Adv. Colloid Interface Sci. *235* (2016) 90–107, https://doi.org/10.1016/j.cis.2016.06.002.
[5] J. Yoreo, P. Vekilov, Principles of crystal nucleation and growth, Rev. Miner. Geochem. *54* (2003) 57–93, https://doi.org/10.2113/0540057.
[6] J. Dirksen, T. Ring, Fundamentals of crystallization: Kinetic effects on particle size distributions and morphology, Chem. Eng. Sci. *46* (1991) 2389–2427, https://doi.org/10.1016/0009-2509(91)80035-W.
[7] A. Sharma, V. Tyagi, C. Chen, D. Buddhi, Review on thermal energy storage with phase change materials and applications, Renew. Sustain. Energy Rev. *13* (2009) 318–345, https://doi.org/10.1016/j.rser.2007.10.005.
[8] N. Denkov, S. Tcholakova, I. Lesov, D. Cholakova, S. Smoukov, Self-shaping of oil droplets via the formation of intermediate rotator phases upon cooling, Nature *528* (2015) 392–395, https://doi.org/10.1038/nature16189.
[9] Evans, E.; Skalak, R. (Eds.) Mechanics and Thermodynamics of Biomembranes. CRC Press: Boca Raton, 1980. doi: 10.1201/9781351074339; eBook ISBN: 9781351074339.
[10] D. Cholakova, Z. Valkova, S. Tcholakova, N. Denkov, S. Smoukov, Self-shaping" of multicomponent drops, Langmuir *33* (2017) 5696–5706, https://doi.org/10.1021/acs.langmuir.7b01153.
[11] S. Tcholakova, Z. Valkova, D. Cholakova, Z. Vinarov, I. Lesov, N. Denkov, S. Smoukov, Efficient self-emulsification via cooling-heating cycles, Nat. Commun. *8* (2017) 15012, https://doi.org/10.1038/ncomms15012.

[12] Z. Valkova, D. Cholakova, S. Tcholakova, N. Denkov, S. Smoukov, Mechanisms and control of self-emulsification upon freezing and melting of dispersed alkane drops, Langmuir *33* (2017) 12155–12170, https://doi.org/10.1021/acs.langmuir.7b02048.
[13] D. Cholakova, N. Denkov, Rotator phases in alkane systems: in bulk, surface layers and micro/nano-confinements, Adv. Colloid Interface Sci. *269* (2019) 7–42, https://doi.org/10.1016/j.cis.2019.04.001.
[14] E. Sirota, A. Herhold, Transient phase-induced nucleation, Science *283* (1999) 529–532, https://doi.org/10.1126/science.283.5401.529.
[15] M. Broadhurst, An analysis of the solid phase behavior of the normal paraffins, J. Res. Natl. Bur. Stand. Sect. A 66A (1962) 241–249.
[16] Y. Shinohara, N. Kawasaki, S. Ueno, I. Kobayashi, M. Nakajima, Y. Amemiya, Observation of the transient rotator phase of n-hexadecane in emulsified droplets with time-resolved two-dimensional small- and wide-zngle X-ray scattering, Phys. Rev. Lett. *94* (2005) 097801, https://doi.org/10.1103/PhysRevLett.94.097801.
[17] Y. Shinohara, T. Takamizawa, S. Ueno, K. Sato, I. Kobayashi, M. Nakajima, Y. Amemiya, Microbeam X-ray diffraction analysis of interfacial heterogeneous nucleation of n-hexadecane inside oil-in-water emulsion droplets, Cryst. Growth Des. *8* (2008) 3123–3126, https://doi.org/10.1021/cg701018x.
[18] P. Mukherjee, Phase transitions among the rotator phases of the normal alkanes: a review, Phys. Rep. *588* (2015) 1–54, https://doi.org/10.1016/j.physrep.2015.05.005.
[19] K. Esselink, P. Hilbers, B. van Beest, Molecular dynamics study of nucleation and melting of n-alkanes, J. Chem. Phys. *101* (1994) 9033–9041, org/10.1063/1.468031.
[20] S. Whittington, D. Chapman, Monte Carlo study of rotational premelting in crystals of long chain paraffins, Trans. Faraday Soc. *61* (1965) 2656–2660, https://doi.org/10.1039/TF9656102656.
[21] M. Mazo, E. Oleynilk, N. Balabaev, L. Lunevskaya, A. Grivtsov, Molecular dynamic simulation of motion in solid polymers. Rotator phase of n-alkane, Polym. Bull. *12* (1984) 303–309, https://doi.org/10.1007/BF00263143.
[22] M Klein, Computer simulation studies of solids, Ann. Rev. Phys. Chem. *36* (1985) 525–548, https://doi.org/10.1146/annurev.pc.36.100185.002521.
[23] J.-P. Ryckaert, M. Klein, Translational and rotational disorder in solid nalkanes: constant temperature-constant pressure molecular dynamics calculations using infinitely long flexible chains, J. Chem. Phys. *85* (1986) 1613–1620, https://doi.org/10.1063/1.451203.
[24] J.-P. Ryckaert, M. Klein, I. McDonald, Disorder at the bilayer interface in the pseudohexagonal rotator phase of solid n-alkanes, Phys. Rev. Lett. *58* (1987) 698–701, https://doi.org/10.1103/PhysRevLett.58.698.
[25] J.-P. Ryckaert, I. McDonald, M. Klein, Disorder in the pseudohexagonal rotator phase of n-alkanes: molecular-dynamics calculations for tricosane, Mol. Phys. *67* (1989) 957–979, https://doi.org/10.1080/00268978900101561.
[26] J.-P. Ryckaert, M Klein, I. McDonald, Computer simulations and the interpretation of incoherent neutron scattering experiments on the solid rotator phases of long-chain alkanes, Mol. Phys. *83* (1994) 439–458, https://doi.org/10.1080/00268979400101361.
[27] R. Martonak, W. Paul, K. Binder, Orthorhombic phase of crystalline polyethylene: a Monte Carlo study, J. Chem. Phys. *106* (1997) 8918–8930, https://doi.org/10.1063/1.473955.
[28] S. Fujiwara, T. Sato, Molecular dynamics simulation of structure formation of short chain molecules, J. Chem. Phys. *110* (1999) 9757–9764, https://doi.org/10.1063/1.478941.
[29] I.-E. Mavrantza, D. Prentzas, V. Mavrantza, C. Galiotis, Detailed atomistic molecular-dynamics simulation of the orthorhombic phase of crystalline polyethylene and alkane crystals, J. Chem. Phys. *115* (2001) 3937–3950, https://doi.org/10.1063/1.1386912.
[30] W.-N. Shen, P. Monson, Solid-fluid equilibrium in a nonlinear hard sphere triatomic model of propane, J. Chem. Phys. *103* (1995) 9756–9762, https://doi.org/10.1063/1.469939.
[31] A. Malanoski, P. Monson, The phase behavior of a hard sphere chain model of a binary n-alkane mixture, J. Chem. Phys. *112* (2000) 2870–2877, https://doi.org/10.1063/1.480861.
[32] T. Phillips, S. Hanna, Simulations of the mobile phase of polyethylene, Polymer *46* (2005) 11035–11050, https://doi.org/10.1016/j.polymer.2005.09.019.
[33] T. Yamamoto, Computer simulation of the crystal/melt interface in n-alkane with implication for polymer crystallization, J. Chem. Soc. Faraday Trans. *91* (1995) 2559–2564, https://doi.org/10.1039/FT9959102559.
[34] M. Cao, P. Monson, Solid-fluid and solid-solid phase equilibrium in a model of n-alkane mixtures, J. Chem. Phys. *120* (2004) 2980–2988, https://doi.org/10.1063/1.1637332.
[35] M. Cao, P. Monson, Solid-fluid and solid-solid equilibrium in hard sphere united atom models of n-alkanes: rotator phase stability, J. Phys. Chem. B *113* (2009) 13866–13873, https://doi.org/10.1021/jp902887w.
[36] A. Marbeuf, R. Brown, Molecular dynamics in n-alkanes: premelting phenomena and rotator phases, 054901-1-9, J. Chem. Phys. *124* (2006), https://doi.org/10.1063/1.2148909.
[37] N. Wentzel, S. Milner, Crystal and rotator phases of n-alkanes: a molecular study, 044901-1-10, J. Chem. Phys. *132* (2010), https://doi.org/10.1063/1.3276458.
[38] N. Wentzel, S. Milner, Simulation of multiple ordered phases in C23H48 n-alkane, 224504-1-11, J. Chem. Phys. *134* (2011), https://doi.org/10.1063/1.3589417.
[39] S. Milner, N. Wentzel, Twist solitons in ordered phases of n-alkanes, Soft Matter *7* (2011) 7477–7492, https://doi.org/10.1039/C1SM05326D.
[40] E. Zubova, N. Balabaev, A. Musienko, E. Gusarova, M. Mazo, L. Manevitch, A. Berlin, Simulation of melting in crystalline polyethylene, 224906-1-12, J. Chem. Phys. *136* (2012), https://doi.org/10.1063/1.4728112.
[41] F. Frank, J. van der Merwe, One-dimensional dislocations: static theory, Proc. R. Soc. Lond. Ser. A *198* (1949) 205–216, https://doi.org/10.1098/rspa.1949.0095.
[42] D. Doherty, A. Hopfinger, Molecular modeling of polymers: molecular dynamics simulation of the rotator phase of C21H44, Phys. Rev. Lett. *72* (1994) 661–664, https://doi.org/10.1103/PhysRevLett.72.661.
[43] Z. Rao, S. Wang, F. Peng, Self diffusion and heat capacity of n-alkanes based phase change materials: a molecular dynamics study, Int. J. Heat Mass Transf. *64* (2013) 581–589, https://doi.org/10.1016/j.ijheatmasstransfer.2013.05.017.
[44] Z. Rao, S. Wang, Y. Zhang, Molecular dynamics simulations of phase transition of n-nonadecane under high pressure, Phase Transit *85* (2012) 400–408, https://doi.org/10.1080/01411594.2011.634331.
[45] Y. Tsuchiya, H. Hasegawa, T. Iwatsubo, Prediction of the melting point of n-alkanes using the molecular dynamics method, J. Chem. Phys. *114* (2001) 2484–2488, https://doi.org/10.1063/1.1338508.
[46] Y. Tsuchiya, H. Hasegawa, T. Iwatsubo, Prediction of the latent heat of n-alkanes using the molecular dynamics method, J. Appl. Phys. *42* (2003) 6508, https://doi.org/10.1143/JJAP.42.6508.
[47] F. Guillaume, J. Ryckaert, V. Rodriguez, L. Mac Dowell, P. Girard, A. Dianoux, Molecular dynamics in solid n-nonadecane: experiments and computer simulations, Phase Transit *76* (2003) 823–830, https://doi.org/10.1080/01411590310001613707.
[48] A. Burrows, I. Korotkin, A. Smoukov, E. Boek, A. Karabasov, Benchmarking of molecular dynamics force fields for solid–liquid and solid–solid phase transitions in alkanes, J. Phys. Chem. B *125* (2021) 5145–5159, https://doi.org/10.1021/acs.jpcb.0c07587.
[49] D. Tobias, K. Tu, M. Klein, Assessment of all-atom potentials for modeling membranes: molecular dynamics simulations of solid and liquid alkanes and crystals of phospholipid fragments, J. Chim. Phys. Phys. Chim. Biol. *94* (1977) 1482–1502, https://doi.org/10.1051/jcp/1997941482.
[50] S. Iliev, S. Tsibranska, A. Ivanova, S. Tcholakova, N. Denkov, Computational assessment of hexadecane freezing by equilibrium atomistic molecular dynamics simulations, J. Colloid Interface Sci. *638* (2023) 743–757, https://doi.org/10.1016/j.jcis.2023.01.126.
[51] S. Iliev, I. Kichev, S. Tsibranska, A. Ivanova, S. Tcholakova, N. Denkov, Computational procedure for analysis of crystallites in polycrystalline solids of quasilinear molecules, Molecules *28* (2023) 2327, https://doi.org/10.3390/molecules28052327.
[52] G. Bussi, D. Donadio, M. Parrinello, Canonical sampling through velocity rescaling, J. Chem. Phys. *126* (2007) 014101, https://doi.org/10.1063/1.2408420.
[53] H. Berendsen, J. Postma, W. van Gunsteren, A. DiNola, J. Haak, Molecular dynamics with coupling to an external bath, J. Chem. Phys. *81* (1984) 3684–3690, https://doi.org/10.1063/1.448118.
[54] T. Darden, D. York, L. Pedersen, Particle mesh Ewald: an N·log(N) method for Ewald sums in large systems, J. Chem. Phys. *98* (1993) 10089–10092, https://doi.org/10.1063/1.464397.
[55] U. Essmann, L. Perera, M. Berkowitz, T. Darden, H. Lee, L. Pedersen, A smooth particle mesh Ewald method, J. Chem. Phys. *103* (1995) 8577–8593, https://doi.org/10.1063/1.470117.
[56] A. Toukmaji, C. Sagui, J. Board, T. Darden, P.M.E.- Efficient, based approach to fixed and induced dipolar interactions, J. Chem. Phys. *113* (2000) 10913–10927, https://doi.org/10.1063/1.1324708.
[57] U. Essmann, L. Perera, M. Berkowitz, T. Darden, H. Lee, L. Pedersen, A smooth particle mesh Ewald method, J. Chem. Phys. *103* (1995) 8577–8593, https://doi.org/10.1063/1.470117.
[58] J.-P. Ryckaert, G. Ciccotti, H. Berendsen, Numerical integration of the cartesian equations of motion of a system with constraints: molecular dynamics of n-alkanes, J. Comput. Phys. *23* (1977) 327–341, https://doi.org/10.1016/0021-9991(77)90098-5.
[59] S. Miyamoto, P. Kollman, Settle: An analytical version of the SHAKE and RATTLE algorithm for rigid water models, J. Comput. Chem. *13* (1992) 952–962, https://doi.org/10.1002/jcc.540130805.
[60] J. Klauda, R. Venable, J. Freites, J. O'Connor, D. Tobias, C. Mondragon-Ramirez, I. Vorobyov, A. MacKerell Jr., R. Pastor, Update of the CHARMM All-atom additive force field for lipids: validation on six lipid types, J. Phys. Chem. B *114* (2010) 7830–7843, https://doi.org/10.1021/jp101759q.
[61] W. Jorgensen, J. Chandrasekhar, J. Madura, R. Impey, M. Klein, Comparison of simple potential functions for simulating liquid water, J. Chem. Phys. *79* (1983) 926–935, https://doi.org/10.1063/1.445869.
[62] W. Jorgensen, J. Madura, Temperature and size dependence for Monte Carlo simulations of TIP4P water, Mol. Phys. *56* (1985) 1381–1392, https://doi.org/10.1080/00268978500103111.
[63] M. Abraham, T. Murtola, R. Schulz, S. Páll, J. Smith, B. Hess, E. Lindahl, GROMACS: High performance molecular simulations through multi-level parallelism from laptops to supercomputers, Software X *1-2* (2015) 19–25, https://doi.org/10.1016/j.softx.2015.06.001.
[64] W. Humphrey, A. Dalke, K. Schulten, VMD: visual molecular dynamics, J. Mol. Graph. *14* (1996) 33–38, https://doi.org/10.1016/0263-7855(96)00018-5.
[65] P. Jaccard, Nouvelles recherches sur la distribution florale, Bull. Soc. Vaud. Sci. Nat. *44* (1908) 223–270, https://doi.org/10.5169/seals-268384.
[66] S. Craig, G. Hastie, K. Roberts, J. Sherwood, Investigation into the structures of some normal alkanes within the homologous series C13H28 to C60H122 using high-resolution synchrotron X-ray powder diffraction, J. Mater. Chem. 4 (1994) 977–981, https://doi.org/10.1039/JM9940400977.